

UCLA

UCLA Previously Published Works

Title

Magnetostratigraphic dating of the late Miocene Baogeda Ula Formation and associated fauna in central Inner Mongolia, northern China

Permalink

<https://escholarship.org/uc/item/83n375b2>

Authors

Sun, Lu
Deng, Chenglong
Wang, Xiaoming
et al.

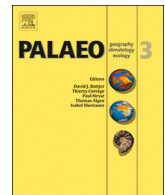
Publication Date

2018-09-01

DOI

10.1016/j.palaeo.2018.06.001

Peer reviewed



Magnetostratigraphic dating of the late Miocene Baogeda Ula Formation and associated fauna in central Inner Mongolia, northern China

Lu Sun^{a,b,c}, Chenglong Deng^{a,b,c,*}, Xiaoming Wang^{d,e,f}, Qian Li^a, Huafeng Qin^{a,b}, Huiru Xu^g, Yanfen Kong^{a,b,c}, Bailing Wu^{a,b,c}, Suzhen Liu^{a,b,c}, Rixiang Zhu^{a,b,c}

^a State Key Laboratory of Lithospheric Evolution, Institute of Geology and Geophysics, Chinese Academy of Sciences, Beijing 100029, China

^b Institutions of Earth Science, Chinese Academy of Sciences, Beijing 100029, China

^c College of Earth and Planetary Science, University of Chinese Academy of Sciences, Beijing 100049, China

^d Department of Vertebrate Paleontology, Natural History Museum of Los Angeles County, 900 Exposition Blvd., Los Angeles 90007, USA

^e Key Laboratory of Evolutionary Systematics of Vertebrates, Institute of Vertebrate Paleontology and Paleoanthropology, Chinese Academy of Sciences, Beijing 100044, China

^f Integrative and Evolutionary Biology Program, Department of Biological Sciences, University of Southern California, Los Angeles 90089, USA

^g Hubei Subsurface Multi-Scale Imaging Key Laboratory, Institute of Geophysics and Geomatics, China University of Geosciences, Wuhan 430074, China

ARTICLE INFO

Keywords:
Magnetostratigraphy

East Asia

Baodean Age

Fluvio-lacustrine sediments

Hipparrison Fauna

ABSTRACT

Detailed understanding to the evolution of Neogene land mammals in East Asia and its intercontinental correlation has been impeded by the absence of an integrated biochronological system of this region. The numerous and diverse records of Neogene vertebrate fossils preserved in Inner Mongolia of northern China play a key role in the establishment of an independent biochronological framework in East Asia. However, most of these faunas are poorly constrained by independent chronological controls due to the scattered distribution of fossil localities and insufficient exposure of the fossiliferous strata. Additionally, age estimates by mammalian evolution and correlation often have uncertainties greater than ~1–2 million years. Here we present new magnetostratigraphic results of the Baogeda Ula Fauna, which was generally assigned an early Baodean Age (Late Miocene), or equivalent to the European MN12 zone (middle Turolian). *Hipparrison* remains and associated vertebrate fossils were excavated from the upper part of the fluvio-lacustrine Baogeda Ula Formation near Abaga Banner, central Inner Mongolia of northern China. At least two layers of basalt sheet flows can be observed on top of the Baogeda Ula Formation. Our magnetostratigraphy, aided by published biochronology data and K-Ar ages of the lower basalt layer suggests that the Baogeda Ula Fauna consisting of three fossiliferous horizons can be placed within chron C4n.1n with an age range of 7.642–7.528 Ma. Thus, the Baogeda Ula Fauna becomes the first and only Baodean assemblage that is constrained by both magnetostratigraphy and radiometric ages, offering an anchoring point for future biochronological correlations.

1. Introduction

The biostratigraphy based on mammal fossils has proved useful to date and correlate Cenozoic terrestrial sediments among different continents (Wang et al., 2013; Deng et al., 2018b). However, the discontinuous nature of the vertebrate fossils in both temporal and spatial dimensions restricts a wide application in chronostratigraphy. Moreover, the endemism and asynchrony of mammalian dispersal and evolution in various geographic regions strongly influence the land mammal chronological systems in different continents. Great strides have been made on a system of Asian Neogene mammalian biostratigraphy from efforts of more than a century. Nevertheless, compared

with Europe and North America, Asian Neogene bio-chronostratigraphic framework needs to be further refined in both division and age constraints of the biozones.

Being geographically between Europe and North America and possessing abundant mammal fossil localities, East Asia is an ideal area to achieve this goal. Based on pioneering discoveries, consecutive Neogene land mammal biochronological systems in northern China have been achieved with the aid of intercontinental faunal correlation (e.g., Qiu and Qiu, 1995; Deng, 2006; Wang et al., 2013; Deng et al., 2018b). According to the latest division of the Chinese Regional Stratigraphic Chart (All-China Stratigraphic Commission, 2017), seven Neogene Land Mammal Stages/Ages (LMS/As) were included: Xiejian,

* Corresponding author at: Institute of Geology and Geophysics, Chinese Academy of Sciences, No. 19, Beihucheng Western Road, Chaoyang District, 100029 Beijing, China.
E-mail address: cldeng@mail.igcas.ac.cn (C. Deng).

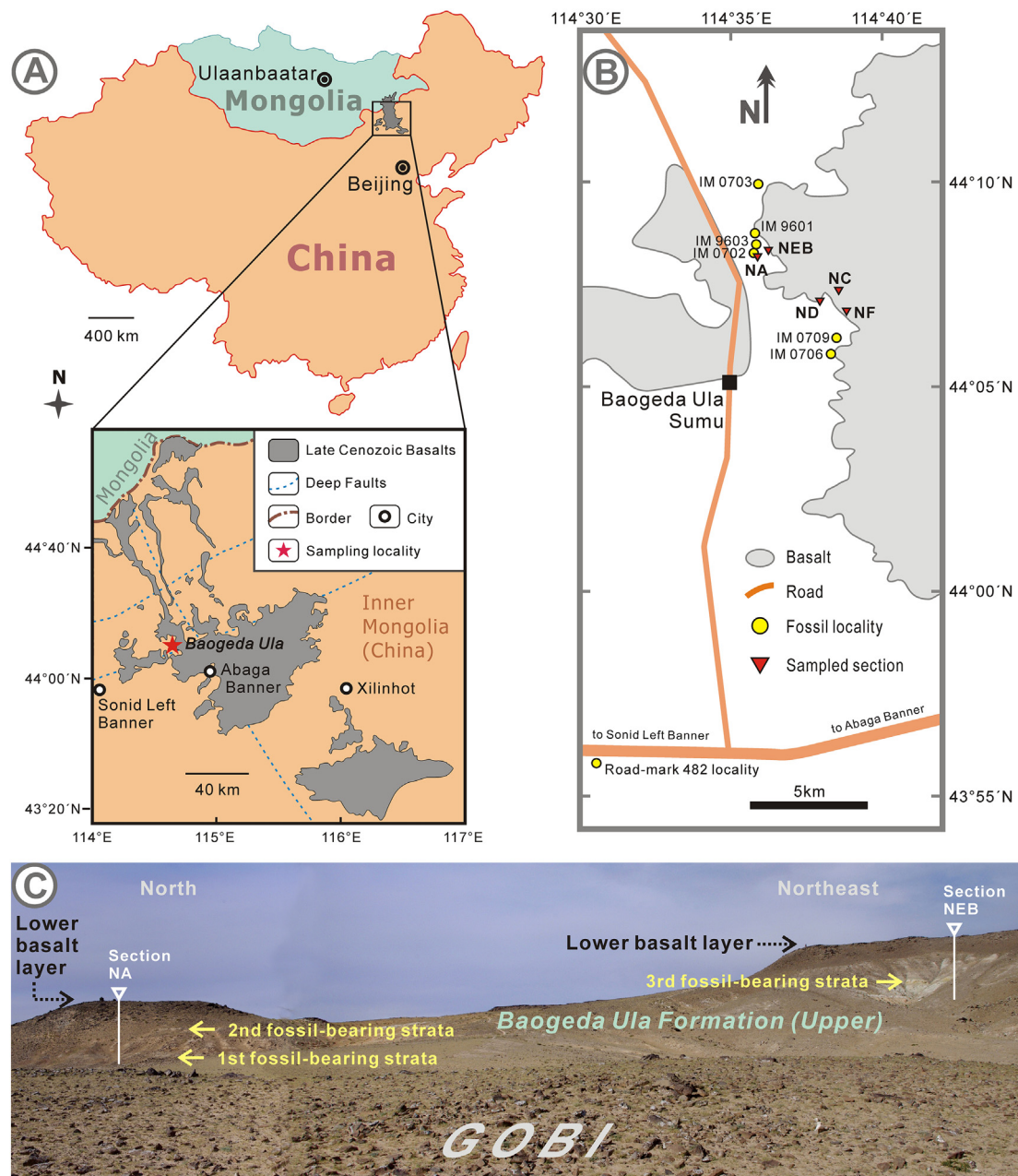


Fig. 1. A) Distribution of the late Cenozoic basalt outcrops in Mongolia and northern China and the schematic geological maps showing the sample location near Abaga Banner, Inner Mongolia (modified from Deng and MacDougal, 1992; Ho et al., 2008). B) Locations of the five sampled sections and some major fossil sites near Baogeda Ula Sumu. C) Macroscopic view of the three fossiliferous horizons near Baogeda Ula Sumu and the capping basalt above Baogeda Ula Formation. The locations of the NA and NEB sections are indicated by the white triangles and vertical lines.

Shanwangian, Tunggurian, Bahean, Baodean, Gaozhuangian, and Mazingouan. One major deficiency of the system remains: few of the boundaries of the LMAs (e.g., the Late Miocene Bahean/Baodean Ages) were well constrained in absolute age (Qiu et al., 2013b; Wang et al., 2013).

During the Late Miocene, mammals became more modernized than their earlier ancestors and are often represented by highly abundant records in northern China (Qiu and Li, 2005). Since nearly a hundred years ago, numerous late Cenozoic vertebrate fossil localities were uncovered from Inner Mongolia Autonomous Region (also known as “Nei Mongol”, hereinafter referred to as “Inner Mongolia”) of northern China (Andersson, 1923; Teilhard de Chardin, 1926; Andrews, 1932). Although the Neogene mammal sites in Inner Mongolia are relatively uninterrupted in temporal dimension (Qiu et al., 2006), most of them

are spatially scattered with scanty stratigraphic exposures and limited thickness. Biochronology based on faunal correlation is generally used in the establishment of the chronological sequence of these faunas (Qiu and Wang, 1999; Qiu et al., 2006). A well-constrained Late Miocene biochronological framework in Inner Mongolia will not only permit a precise age control in the evolutionary history of these terrestrial biota, but also facilitate determination of Bahean/Baodean boundary in Inner Mongolia.

The Neogene terrestrial deposits in northern China are usually fluvial, lacustrine and/or eolian in origin (Wang, 1990; Ding et al., 1998). Due to the absence of datable volcanic rocks within most of these fossiliferous strata, magnetostratigraphy often becomes the only way to constrain their ages (e.g., Guo et al., 2002; Deng et al., 2008, 2018a; Zhu et al., 2008). Although some of the Neogene faunas in Inner

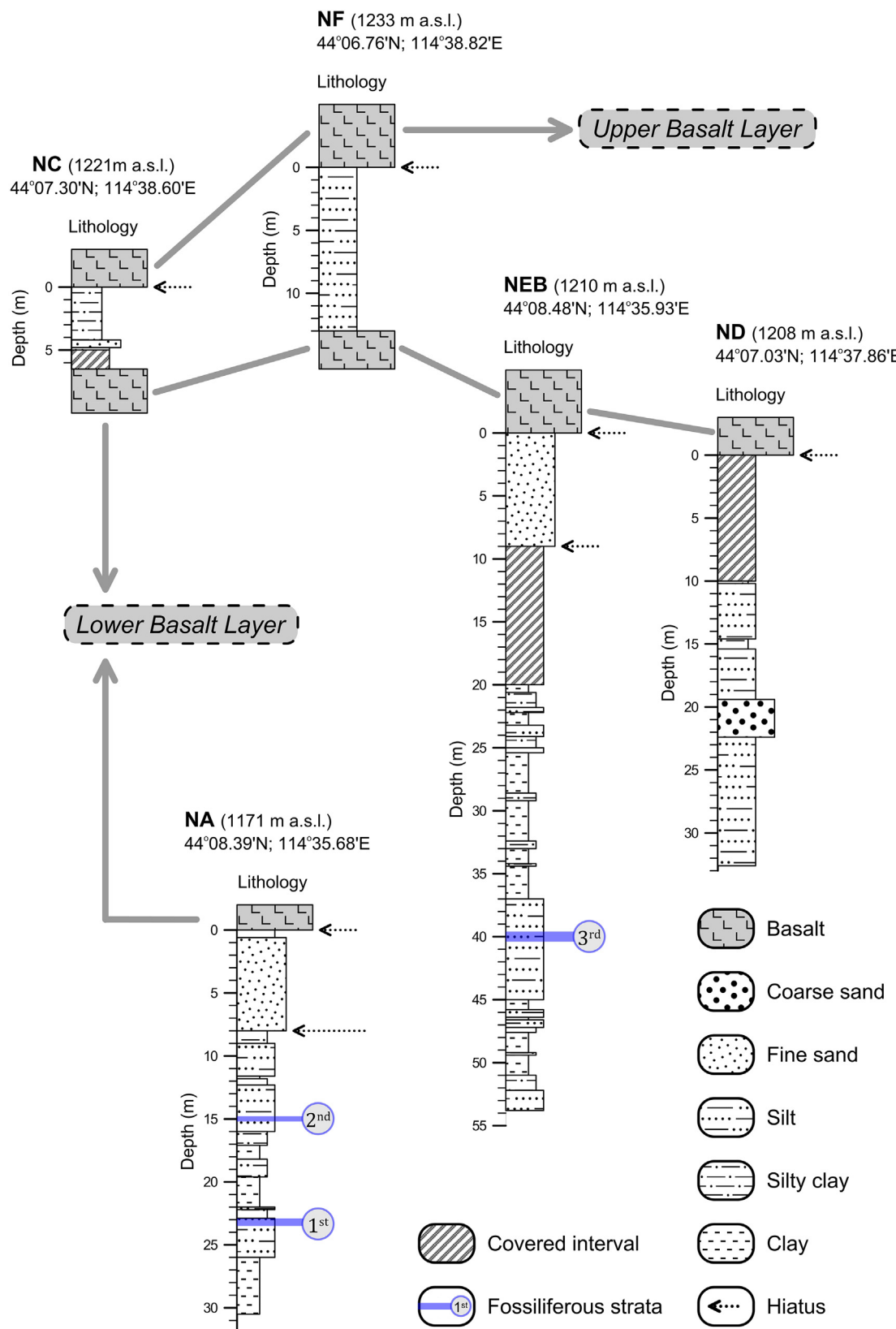


Fig. 2. Lithostratigraphic columns and elevations of the five sections of this study. The arrows with dotted lines indicate the observed or potential unconformity between the two basalt layers and the underlying fluvio-lacustrine sediments.

Mongolia had been paleomagnetically dated (e.g., Wang et al., 2003; Liddicoat et al., 2007; Xu et al., 2007; O'Connor et al., 2008; Kaakinen et al., 2015), the boundary of the Late Miocene Bahean/Baodean Ages

is still undetermined so far.

In central Inner Mongolia, Amuwusu, Shala, Baogeda Ula (also spelled as “Baogedawula”) and Ertemte are four representative

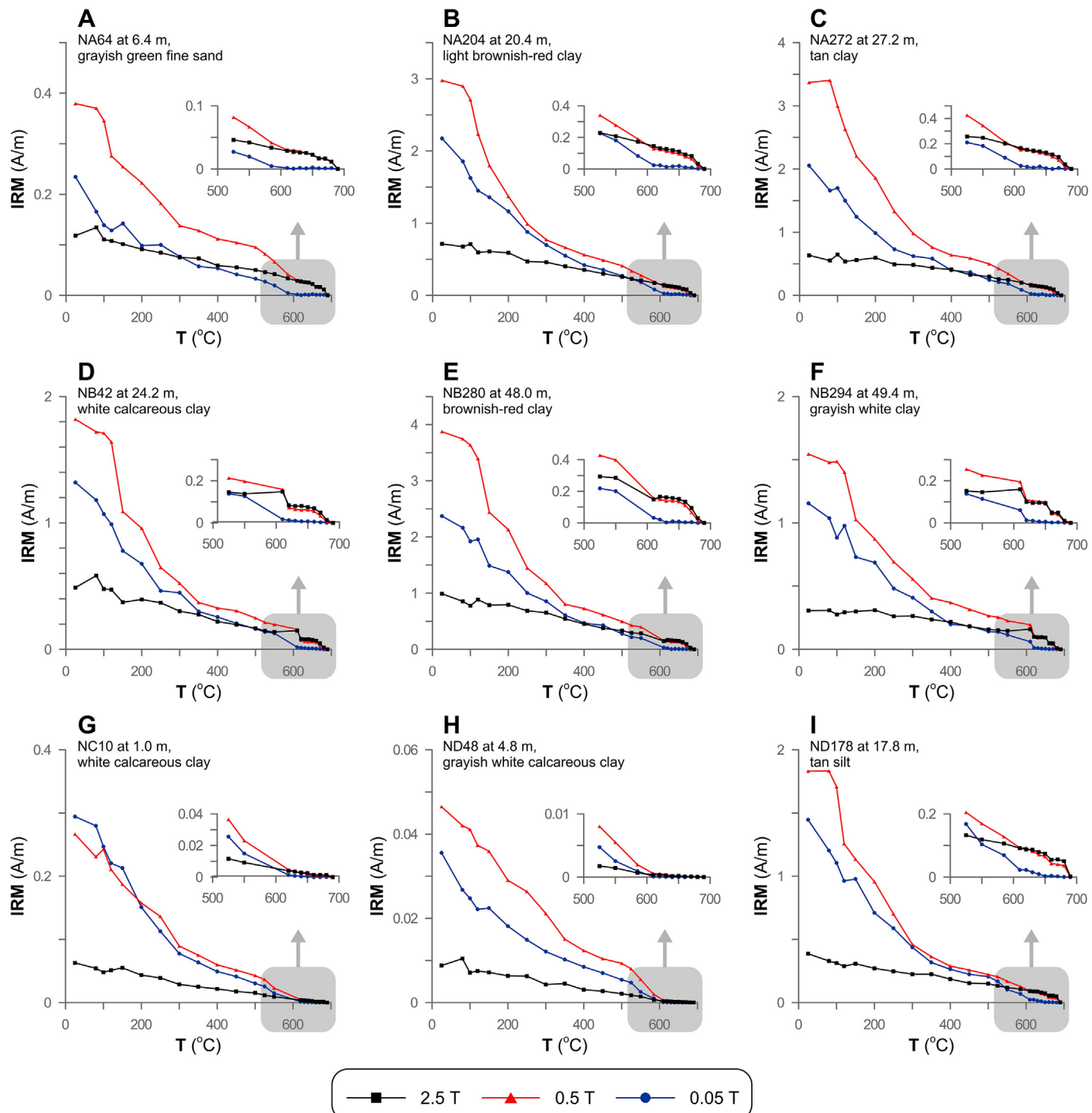


Fig. 3. Progressive thermal demagnetization of a composite IRM (Lowrie, 1990) performed on magnetizing specimens with different lithologies from the investigated Baogeda Ula sections in 2.5, 0.5, 0.05 T along three mutually orthogonal axes, respectively.

localities yielding abundant Late Miocene mammalian faunas (Qiu et al., 2006). However, only in the Baogeda Ula site is at least one basaltic lava sheet closely associated with the fossiliferous sedimentary sequence, an ideal circumstance to ascertain the ages of the strata and associated fauna. In this study we present the magnetostratigraphy of the upper part of the Baogeda Ula Formation and provide an accurate chronological constraint for the Baogeda Ula Fauna combined with the previously published biochronologic and geochronologic data.

2. Geological setting and sampling

Both the Baogeda Ula Formation and fauna of the same name are named after Baogeda Ula Sumu of Abaga (also spelled as “Abag”) Banner, Xilin Gol League in the central Inner Mongolia of northern China (Fig. 1A–B). In Inner Mongolia, Sumu, Banner and League are township-, county- and region-level administrative divisions.

An extensive tableland formed by flat-lying fluvio-lacustrine deposits capped by basaltic lava sheets covers an area of more than a thousand square kilometers around Abaga Banner (Fig. 1A). Three productive fossil-bearing horizons (44°08'23.4"N, 114°35'40.7"E) were

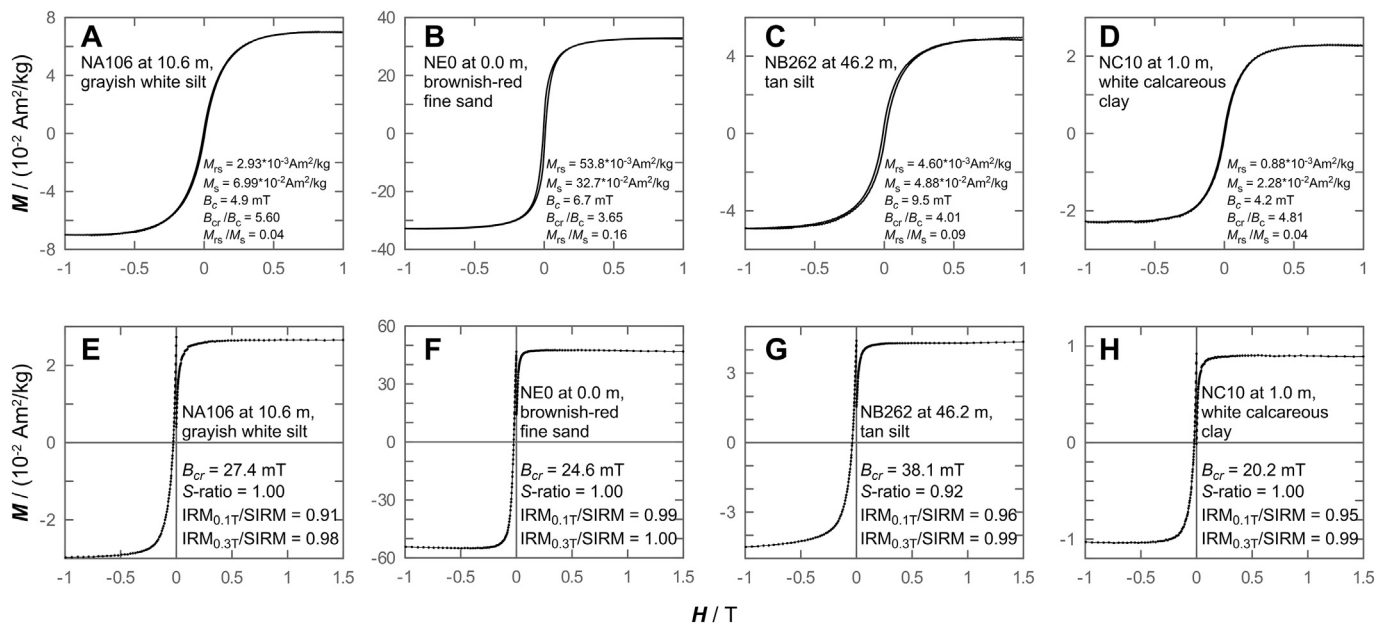


Fig. 4. Hysteresis loops after slope correction for paramagnetic contribution (A, B, C and D) and IRM acquisition and backward-field demagnetization curves (E, F, G and H) of representative specimens from different lithologies at the study site.

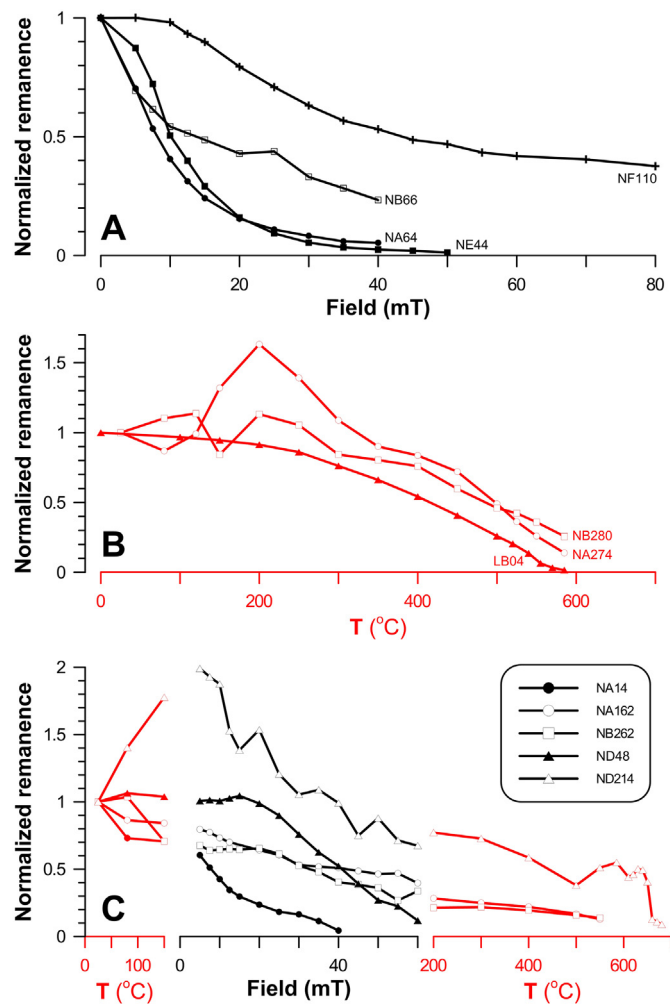


Fig. 5. Remanence decay curves of the natural remanent magnetization (NRM). A) Alternating field (AF) demagnetization curves. B) Thermal demagnetization curves. C) Hybrid demagnetization curves.

unearthed from the outcrop northeast of Baogeda Ula Sumu with a thickness of about 80 m at the western escarpment, which is located about 30 km northwest of the Abaga Banner (Fig. 1B–C). The terrestrial sedimentary sequence, which is mainly composed of interbedded fine sand, silt, silty clay and clay sediments (Fig. 2) of different colors (brown, yellow, grayish-white and grayish-green), belongs to the upper part of the Baogeda Ula Formation. The lower part of the Baogeda Ula Formation does not outcrop in this region. A possible boundary between the Baogeda Ula Formation and underlying Middle Miocene Tunggur Formation can be observed at the Road-mark 482 locality to the southwest of Baogeda Ula Sumu (Wang et al., 2003).

The top of Baogeda Ula Formation is marked by a layer of basaltic lava sheet (with variable thicknesses of 2–15 m) above the sites where fossils were discovered (Fig. 1C). There is a disconformity between the capping basalt layer and the underlying fluvio-lacustrine deposits. Additionally, two layers of basaltic lava can be observed on top of Baogeda Ula Formation around 4 km southeast of the fossil site ($44^{\circ}07'12.1''\text{N}$, $114^{\circ}38'24.3''\text{E}$), where silt/silty clay sediments with thicknesses of about 5–15 m are sandwiched between the two basaltic lava sheets (Supplementary Fig. S1). Several volcanic cones are distributed within and around the vast lava platform. The stratigraphic context of the basalt platform implies multiple volcanic eruptions from several centers in this region (Luo and Chen, 1990).

In order to constrain the age range of the Baogeda Ula Fauna more precisely, we took oriented paleomagnetic hand samples in situ along five sections with a magnetic compass at intervals of 10–20 cm. Two of them, which are named NA and NEB (a combination of two subsections NE and NB), were near the three fossil-bearing sites (Fig. 1B–C). The other three sections, which are named NC, ND, and NF, and are 3–4 km away from the fossil sites, covered the sedimentary interval between and below the two layers of basalt (Fig. 1B, Supplementary Fig. S1). The stratigraphic context and relationship of these sections with the GPS coordinates and elevations above sea level (a.s.l.) are shown in Fig. 2. Although no depositional hiatus was logged during sampling within the sedimentary strata, we inferred that there should be a gap between the fine-grained silt/clay sediments and overlying coarse sand sediments based on the erosive nature of the latter in sections NA, NEB and ND (Fig. 2). The contact surface between basalt layers and the underlying fluvio-lacustrine deposits is interpreted as an unconformity (Fig. 2), because it is hard for the unconsolidated sand/silt sediments to resist

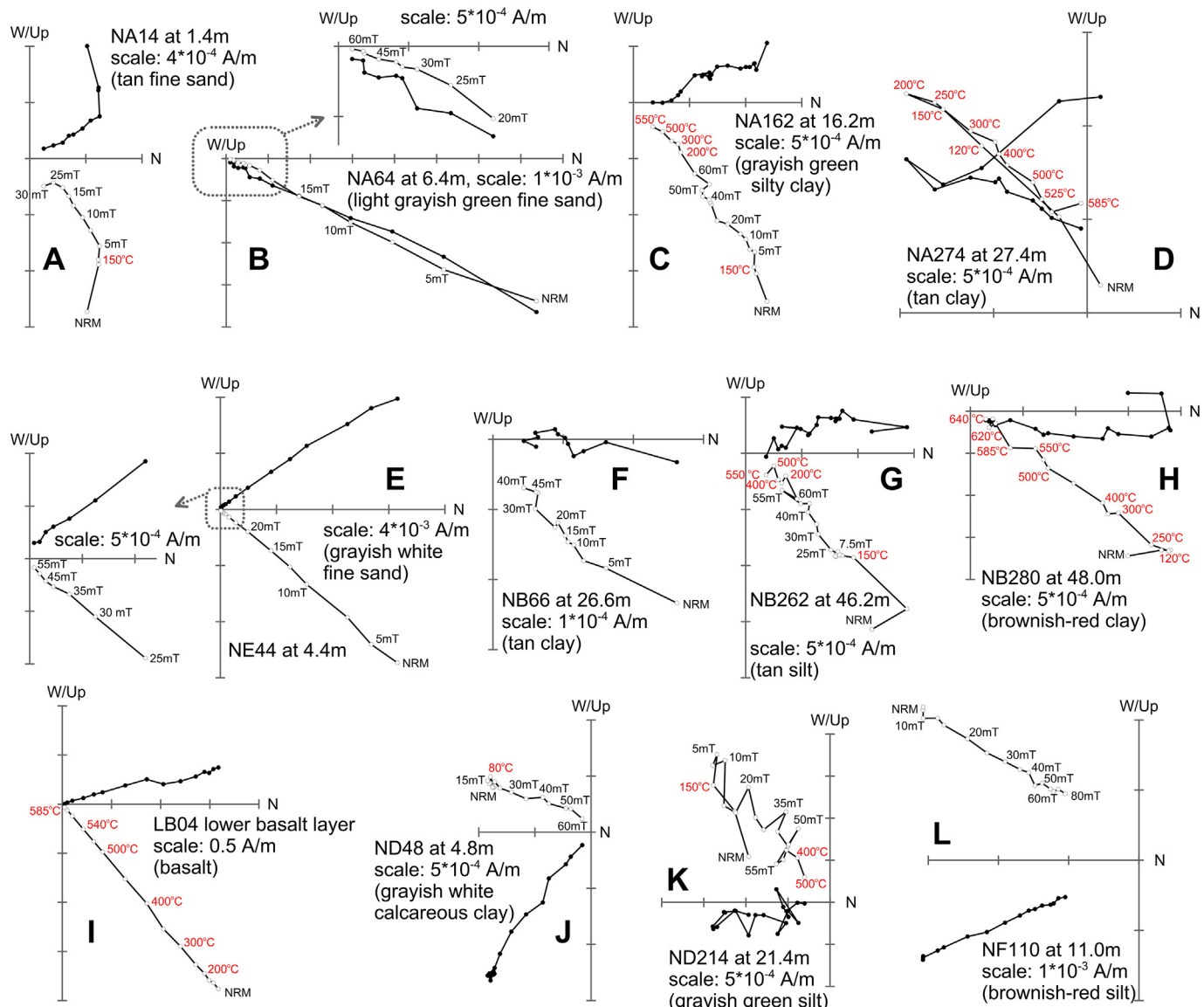


Fig. 6. Orthogonal projections of stepwise demagnetization. The solid (open) circles represent the projection on the horizontal (vertical) planes. The numbers refer to the temperature in °C or alternating field intensity in mT. NRM is the natural remanent magnetization.

the denudation of the dynamic basaltic lava flow from the geological point of view. It is noteworthy that section NA is on the edge of the tableland (Fig. 1C), and its capping basalt layer is distinctly lower (1171 m a.s.l.) than that of other sections (> 1200 m a.s.l.) on the lava platform (Fig. 2).

The sedimentary intervals, which are in close contact (< 2 m) with the capping basalt, were skipped during sampling to avoid potential thermal alteration. Sediments composed of coarse-grained sands or covered by thick basaltic gravels and vegetation were not sampled either. In the laboratory, block sample from each sampling level was fashioned into two or three cubic specimens with faces of 2 cm length.

We also collected eight cylindrical cores from the lower basalt layer with a hand-held gasoline-powered drill. The cores were oriented using both a sun and magnetic compasses in the field and then were cut into several specimens of 2.2 cm in length in the laboratory.

3. Rock magnetic properties

3.1. Methodology

To identify the nature of the magnetic carrier(s) in the sediments, a series of rock magnetic analysis were performed before stepwise demagnetization. Thermal demagnetization of three-component isothermal remanent magnetization (IRM), hysteresis parameters, IRM acquisition curves and direct current (DC) field demagnetization of the saturated IRM (SIRM), were carried out on a selection of specimens from different types of lithologies.

The composite IRMs of the cubic specimens were acquired in DC fields of 2.5 T (high-coercivity or hard component), 0.5 T (medium coercivity component) and 0.05 T (low-coercivity or soft component) along three mutually orthogonal axes, respectively (Lowrie, 1990), with a 2G Enterprises Pulse Magnetizer (2G-660). They were then thermally demagnetized up to 690 °C from room temperature (20 °C) at 10–50 °C intervals after 24 heating steps using a thermal demagnetizer (ASC Scientific Model TD-48).

Hysteresis properties were measured with a MicroMag 3900

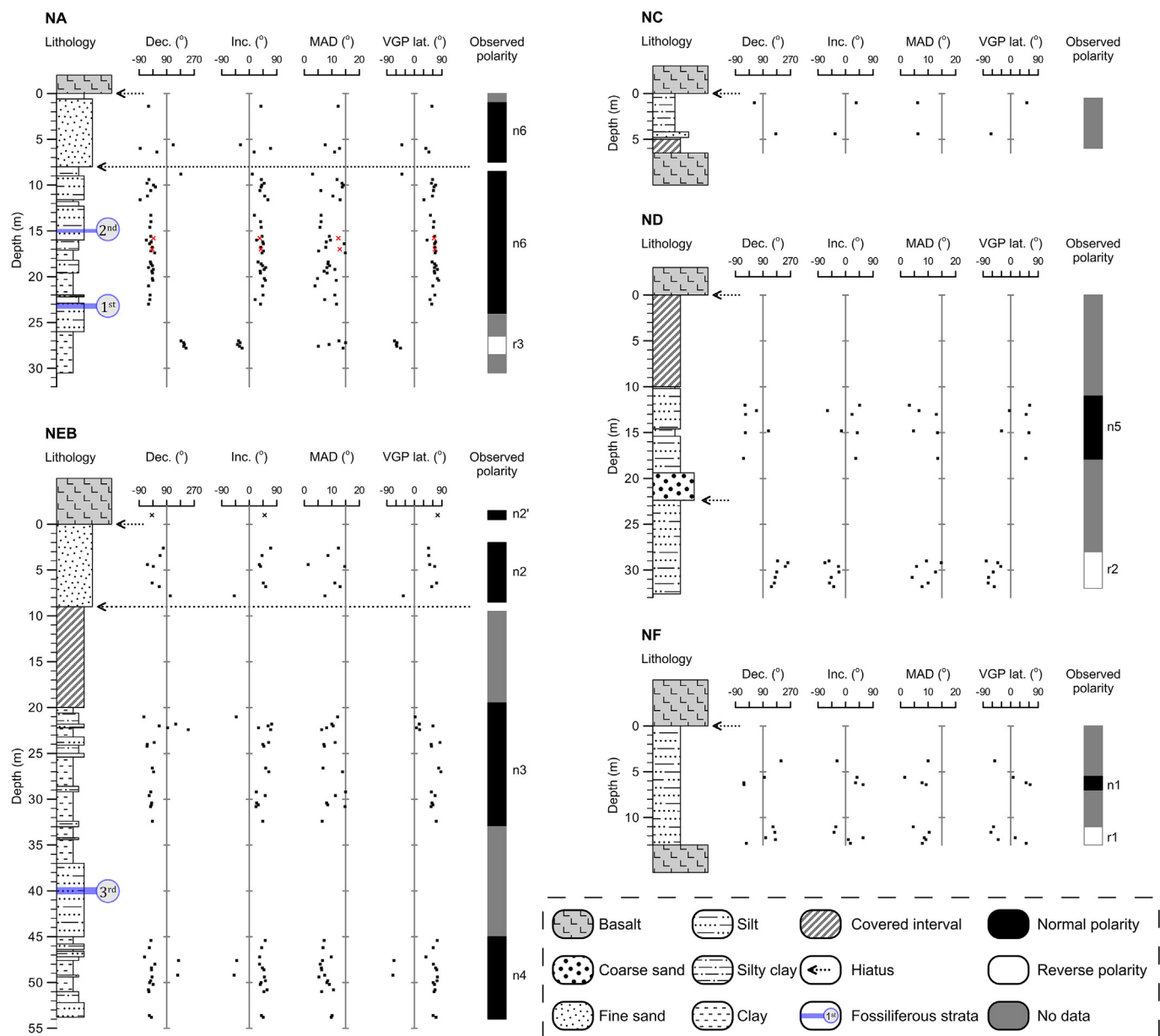


Fig. 7. Lithostratigraphy and palaeomagnetic results of the five studied sections. Specimen take magnetite (haematite) as their major ChRM carrier is symbolized by square (cross). Dec., declination; Inc., inclination; MAD, maximum angular deviation (with cut-off at 15°); VGP, virtual geomagnetic pole.

Vibrating Sample Magnetometer (VSM) (Princeton Measurements Corp., NJ, USA). The magnetic fields cycled between ± 1.0 T. Saturation magnetization (M_s), saturation remanence (M_{rs}) and coercivity (B_c) were determined after correction for the paramagnetic contribution identified from the slope at high fields. The SIRM of the specimens were imparted from 0 to 1.5 T after demagnetizing in an alternating field (AF) up to 1.5 T. They were subsequently exposed to reverse fields of increasing intensities up to 1.0 T to obtain the coercivity of remanence (B_{cr}).

3.2. Rock magnetic results

As shown by the thermal demagnetization curves of the three-component IRM (Fig. 3), remarkable slope changes of the soft components at 585 °C imply that magnetite is ubiquitous in the sediments. Another slight slope changes of the low-coercivity components around 250–300 °C (Fig. 3B, C, D and G) may be caused by the conversion of metastable maghemite. The remanence intensities of the hard- and

medium-components of some specimens (Fig. 3A, E, F and I) drop to zero up to about 680 °C, which is the unblocking temperature of haematite.

All 16 selected specimens display similar shapes of hysteresis loops which saturate above 0.3 T with relatively small M_{rs}/M_s ratios lower than 0.26 (Fig. 4A–D). IRM acquisition curves and DC field demagnetization of the SIRM show high S -ratios of > 0.84 (Fig. 4E–H). Meanwhile, the hysteresis ratios (M_{rs}/M_s vs. B_{cr}/B_c) indicate that the magnetic minerals are characterized by pseudo-single-domain (PSD) grains (Day et al., 1977). These results also reveal the dominance of low-coercivity ferrimagnetic components, which is magnetite, in the sediments.

Based on these rock magnetic results, we conclude that magnetite is the dominant magnetic carrier in the sediments of Baogeda Ula Formation. Haematite and maghemite are also identified from a few specimens.

Table 1

Interpretive paleomagnetic results of the five studied sections and the composite section.

| Section name | Depth interval/m | Polarity |
|-------------------|--------------------------------|---------------|
| NA | 0–1.4 | Undefined |
| | 1.4–23.0 | Normal (n6) |
| | 23.0–27.0 | Undefined |
| | 27.0–27.8 | Reversed (r3) |
| | 27.8–30.5 | Undefined |
| NEB | Lower basalt layer | Normal (n2') |
| | 0–2.6 | Undefined |
| | 2.6–7.8 | Normal (n2) |
| | 7.8–21.0 | Undefined |
| | 21.0–32.4 | Normal (n3) |
| NC | 32.4–45.4 | Undefined |
| | 45.4–53.8 | Normal (n4) |
| | 0–6.0 | Undefined |
| ND | 0–12.0 | Undefined |
| | 12.0–17.8 | Normal (n5) |
| | 17.8–29.0 | Undefined |
| NF | 29.0–32 | Reversed (r2) |
| | 0–5.6 | Undefined |
| | 5.6–6.4 | Normal (n1) |
| | 6.4–11.0 | Undefined |
| Composite section | 11.0–13.0 | Reversed (r1) |
| | 0–6 | Undefined |
| | 6.0–8.0 | Normal (N1) |
| | 8.0–13.0 | Reversed (R1) |
| | Lower basalt layer (13.0–23.0) | Normal (N2) |
| | 23.0–58.0 | Normal (N2) |
| | 58.0–63.0 | Reversed (R2) |
| | 63.0–78.0 | Normal (N3) |
| | 78.0–93.0 | Reversed (R3) |

4. Magnetostatigraphic results

4.1. Demagnetization of the nature remanent magnetization (NRM)

According to the conclusion derived from the rock magnetic measurements, most of the specimens were demagnetized by 14 incremental alternating field (AF) steps up to 80 mT at 2.5–10 mT intervals (Fig. 5A). The rest of them were thermally demagnetized up to 690 °C (using incremental heating steps of 25–50 °C below and 10–25 °C above 585 °C) (Fig. 5B) from room temperature (20 °C) with a Magnetic Measurements Thermal Demagnetizer (MMTD Model 80) installed in a magnetically shielded space (< 300 nT). To the few specimens which failed to yield significant results after AF demagnetization or insufficiently demagnetized up to 80 mT, reserved specimens from the same stratigraphic level were subsequently subject to hybrid demagnetization. They were thermally demagnetized from room temperature (20 °C) to 150 °C to remove the secondary remanence then followed by AF demagnetization up to a peak field of 60 mT at 2.5–10 mT intervals. AF demagnetization is effective in isolating the characteristic remanent magnetization (ChRM) in these sediments without causing magnetic mineral phases transformation during heating. Some of them were ultimately thermal-demagnetized up to 585 °C or 690 °C after AF demagnetization, as appropriate (Fig. 5C). For the basalt samples, one specimen was chosen from each core to conduct thermal demagnetization. In total, eight specimens were thermally demagnetized up to 585 °C from room temperature (20 °C) with heating intervals of 50 °C below and 15–20 °C above 500 °C. Measurements of the NRM and the remanence of all these specimens after each demagnetization step were conducted on a horizontal 2G Enterprises DC SQUID cryogenic magnetometer installed in a magnetically shielded space (< 300 nT). Demagnetization results were evaluated by orthogonal vector diagrams (Zijderveld, 1967).

Stepwise demagnetization diagrams of representative specimens (Fig. 6) revealed the presence of at least two magnetic components. A low field or low temperature viscous remanence was typically removed

between 5 and 20 mT (Fig. 6A, F and J) and at around 250 °C (Fig. 6D and H). Vector diagrams decayed to origin and a high coercivity component, which was isolated between 25 and 80 mT (Fig. 6B, E and L) or above 400 °C (Fig. 6C, G, H, I and K), is interpreted to represent the ChRM direction. The directions of ChRM were subsequently calculated using principal component analysis (Kirschvink, 1980) based on at least four successive demagnetization steps of high field/temperature. Data analyses were carried out in the PaleoMag software developed by Craig H. Jones and Joya Tetreault.

4.2. Magnetostatigraphy

Declination and inclination results of the five sections are plotted by depth in Fig. 7. For the sediment samples, specimens showing maximum angular deviation (MAD) values larger than 15° were considered unreliable and were excluded from the results. A total of 115 (~32% of all the demagnetized specimens) specimens from 105 sedimentary levels yielded reliable ChRM directions (Supplementary Table S1). Each data point from the sediment in Fig. 7 represents the result of one specimen. The relatively coarse grain size of the sediments is suggested to be responsible for the failure of demagnetization to most of the rejected specimens. Only 28.9% (39.4 m) of the five sections consist of fine-grained sediments (clays and silty clays). More than half of the five sections (54.6%) are relatively coarse-grained sediments (silts and sands) by thickness. Specimens from these sediments often show erratic demagnetization behaviors at high field/temperature. No specimen is obtained from the rest of the sections (16.5%) due to the inaccessibility or poor exposure of the strata. For the basalt specimens, more than five demagnetization steps were actually used to calculate vectors for each specimen, and all meet the criterion that MAD values are lower than 5° (Supplementary Table S1).

The latitudes of the virtual geomagnetic pole (VGP) were calculated by the ChRM vector directions (Supplementary Table S1), which were used to define the succession of the geomagnetic polarity sequences of the five sections (Fig. 7, Table 1). The magnetic polarity is defined by the results of at least two successive specimens with same polarity. Section NA consists of at least two magnetozones. A reversed polarity (r3) is recognized from the base of the section whereas the rest is dominantly normal. There is an inconspicuous disconformity within the normal polarity (n6). Section NEB is dominated by three normal polarities (n2, n3 and n4). They are separated by two gray shaded intervals which indicate undetermined polarities. The site-mean direction ($D/I = 353.5^\circ \pm 50.5^\circ, \alpha_{95} = 6.6$) of the eight basalt specimens from the lower basalt layer of section NEB were calculated using Fisher's (1953) statistics. The corresponding VGP latitude (76.1°N) revealed a normal magnetic polarity (n2') of the lower basalt layer. We inferred that the two neighboring normal magnetozones, n2 and n2', probably recorded the same normal chron, although there is an inconspicuous disconformity between them. Section ND contains at least two magneto-zones. The upper half of the section shows a normal polarity (n5) while the lower half shows a reversed polarity (r2).

Sections NC and NF covered the strata between two basaltic lava sheets (Fig. 7). Only two specimens yielded reliable ChRM directions from section NC. The upper specimen is normal while the lower one is reversed in polarity. The scarcity of data makes it impossible to achieve any explicit pattern. The base of the section NF is a reversed polarity (r1) whereas the middle part of the section is normal (n1). There seems to be a reversed polarity above magnetozone n6 but this reversal is defined by only one specimen.

Considering the horizontal sedimentary strata with no discernable tilt and the relative elevational differences of the five sections (Fig. 2), the obtained polarities in Fig. 7 can be integrated into a single geomagnetic polarity sequence (Fig. 8, Table 1). The sediments between two basalt layers recorded at least two polarities based on the results from section NF. The lower part (r1) is reversed (R1) and the upper one (n1) is normal (N1) in the composite polarity. Below R1 there is a

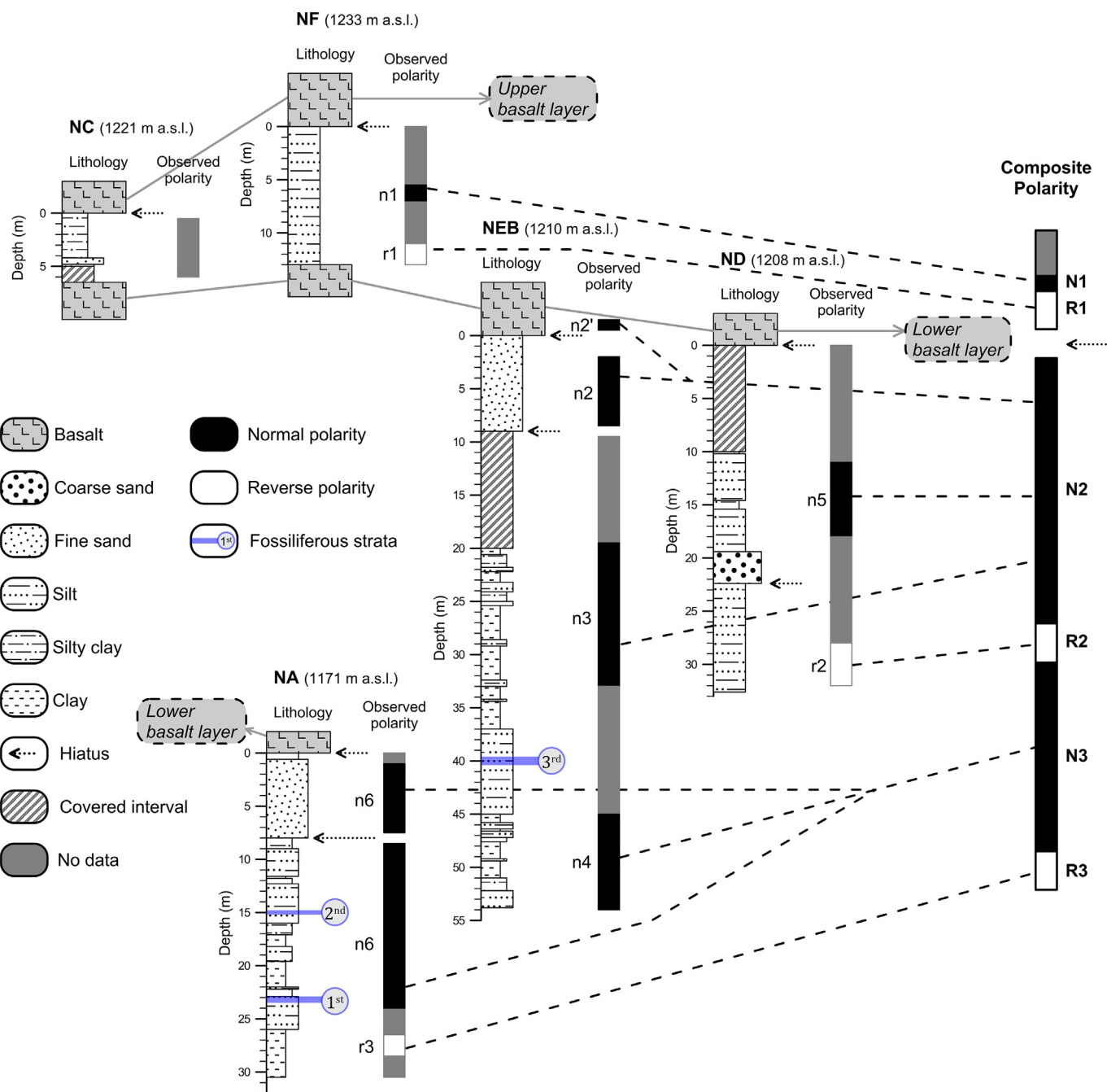


Fig. 8. Integrated magnetostratigraphy based on the palaeomagnetic results derived from the five studied sections.

Table 2

Whole-rock K–Ar dating results of the lower basalt layer near Baogeda Ula Sumu.

| Sample ID | Latitude (degrees) | Longitude (degrees) | Elevation (m.a.s.l.) | Rock type | K (%) | ^{40}Ar rad (mol/g) | ^{40}Ar rad (%) | Age ($\pm 1\sigma$, Ma) | Reference |
|-----------|--------------------|---------------------|----------------------|---------------|-------|------------------------------|--------------------------|---------------------------|---------------------|
| B48 | – | – | – | – | 0.84 | 1.04×10^{-11} | 11.72 | 7.11 ± 0.48 | Luo and Chen, 1990 |
| 100916-4 | 43.9849 N | 114.7597 E | 1183 | Alkali basalt | 1.09 | 1.35×10^{-11} | 82.90 | 7.14 ± 0.18 | Zhang and Guo, 2016 |

depositional hiatus marked by the lower basalt layer. It is difficult to estimate the duration of the hiatus. The interval between n2 and n3 in section NEB did not yield reliable data. However, the results from section ND in similar range of depth showed a normal polarity (n5). Thus, we assigned n2, n3, n5, as well as n2' (from the lower basalt layer) above n2, to the same normal polarity N2. The reversed polarity r2 at the bottom of section ND, which is higher in elevation than the top

of section NA, was not recognized in section NEB. This is an individual polarity (R2) above R1 and N1. Polarity r3 at the bottom of section NA should be the earliest magnetozone (R1), while n6 can be correlated to n4 at the base of section NEB (polarity N3 of the composite result).

The sedimentary sequence underlying the lower basalt layer presents predominantly normal polarities (N2 and N3) in the composite magnetostratigraphic column (Fig. 8). Two short reversed polarities

Table 3

Major vertebrate fossil localities in the type section of Baogeda Ula Formation.

| Inner Mongolia fossil localities | Section | Type of mammals | GPS coordinates |
|----------------------------------|------------------------------|------------------------|-----------------------------|
| IVPP IM9601 | Baogeda Ula Fm. type section | Large mammals only | N44° 08.677', E114° 35.738' |
| IVPP IM9602 | Baogeda Ula Fm. type section | | N44° 08.438', E114° 35.635' |
| IVPP IM9603 | Baogeda Ula Fm. type section | | N44° 08.497', E114° 35.777' |
| IVPP IM0701 | Baogeda Ula Fm. type section | | N44° 08.380', E114° 35.730' |
| IVPP IM0702 | Baogeda Ula Fm. type section | | N44° 08.328', E114° 35.667' |
| IVPP IM0704 | Baogeda Ula Fm. type section | Small mammal wash site | N44° 08.409', E114° 35.932' |

Abbreviations: Fm., formation.

Table 4

Mammalian taxa identified from the Baogeda Ula locality (Qiu et al., 2006, 2013a; Qiu and Li, 2016).

| | | |
|--------------------------------|-----------------------------------|------------------------------------|
| Insectivora | Cricetidae | <i>Alilepus</i> sp. |
| Erinaceidae | <i>Kowalskia shalaensis</i> | Ochotonidae |
| Erinaceidae indet. 1 | <i>Nannocricetus primitivus</i> | <i>Ochotona cf. O. lagreli</i> |
| Erinaceidae indet. 2 | <i>Sinocricetus zdanskyi</i> | Carnivora |
| Soricidae | <i>Microtoscopes fahibuschi</i> | Mephitidae |
| <i>Parasoriculus</i> sp. | <i>Rhinocerodon abagensis</i> | <i>Promephitis</i> sp. |
| Rodentia | Gerbillidae | Mustelidae indet. |
| Gliridae | <i>Abudhabia abagensis</i> | <i>Pekania palaeosinensis</i> |
| <i>Miomimus cf. M. sinesis</i> | Muridae | Hyaenidae |
| Castoridae | <i>Hansdebruijnia perpusilla</i> | <i>Hyaenictitherium hyaenoides</i> |
| <i>Dipoides mengensis</i> | <i>Hansdebruijnia pusilla</i> | Perissodactyla |
| Zapodidae | <i>Karnimatooides hipparionus</i> | Equidae |
| <i>Sicista bilkeensis</i> | <i>Micromys chalceus</i> | <i>Hipparrison tchikoicum</i> |
| <i>Lophocricetus xianensis</i> | Myospalacidae | Rhinocerotidae indet. |
| Dipodidae | <i>Prosiphneus eriksoni</i> | Artiodactyla |
| <i>Paralactaga paridens</i> | Family indet. | Giraffidae indet. |
| <i>Brachycirletes tomidai</i> | <i>Pararhizomys hipparionum</i> | Antilopinae |
| <i>Dipus fraudator</i> | Lagomorpha | <i>Gazella</i> sp. 1 |
| | Leporidae | <i>Gazella</i> sp. 2 |

occur in the bottom (R3) and middle part (R2) of the column. The three fossiliferous horizons lie within the upper, middle and lower part of the normal polarity N3, respectively (Fig. 8). The integrated magnetic polarities could be correlated to the Astronomically Tuned Neogene Time Scale of Hilgen et al. (2012) (ATNTS2012).

5. Chronology of the Baogeda Ula Fauna

5.1. The age of the capping basalt sheet

The basaltic platform near Abaga Banner is part of the spacious volcanic fields of Dariganga Plateau which straddles the border between southeastern Mongolia and Inner Mongolia of northern China (Fig. 1A). As the largest Cenozoic lava platform in eastern Asia, Dariganga Plateau is located in the central Asian orogenic belt, which lies between the North China Craton to the south and the Siberian Craton to the north. The volcanic field is predominantly composed of alkali basalt with subordinate tholeitic basalt (Bureau of Geology and Mineral Resources of Nei Mongol Autonomous Region, 1991; Deng and MacDougall, 1992; Kononova et al., 2002; Ho et al., 2008).

The basaltic platforms in Inner Mongolia are concentrated in two neighboring regions, one is near Abaga Banner and the other on the south side of Xilinhot City (Fig. 1A). At least three basaltic tablelands in different elevations, which implies at least three stages of eruption, were identified from the platform near Abaga Banner (Luo and Chen, 1990). The ages of these basalt layers near Abaga Banner range from

Middle Miocene (14.57 Ma, Luo and Chen, 1990) to Early Pleistocene (2.55 Ma, Ho et al., 2008).

At the western margin of the lava platform where the vertebrate fossils are unearthed, at least two layers of basaltic sheet were observed on top of the fluvio-lacustrine sequence. Compared with the upper basalt layer with a limited distribution, the lower one is more traceable and widespread along the western edge of the tableland near Baogeda Ula. Luo and Chen (1990) dated a series of basaltic lava flows near Abaga Banner using K-Ar method. One sample (B48) from Bayanmende north of Abaga Banner yielded an age of 7.11 ± 0.48 Ma (Table 2). This sample location was thought to be contemporary with the lower basalt layer near Baogeda Ula (Luo and Chen, 1990). A more recent K-Ar date of 7.14 ± 0.18 Ma (Table 2) from the alkali basaltic lava flow (1183 m a.s.l.) from south of Baogeda Ula Sumu further supported the previous age estimate (Zhang and Guo, 2016). Thus, the age of the lower basalt layer capping the Baogeda Ula Formation is well constrained to Late Miocene.

5.2. Biochronology of the Baogeda Ula Fauna

Hipparrison remains and associated vertebrate fossils from Baogeda Ula Formation were first reported by Bureau of Geology and Mineral Resources of Nei Mongol Autonomous Region (1991). The age of these fossils was initially assigned to Pliocene. During the following two decades, more materials of vertebrate fossils were excavated from different horizons and sites near Baogeda Ula Sumu (Wang and Li, 2011). Some of these fossils have been described in detail (Storch and Ni, 2002; Tseng and Wang, 2007; Li, 2010; Wang et al., 2011; Wang et al., 2012; Deng et al., 2016). Tables 3 and 4 list major fossil localities in the type section of Baogeda Ula Formation and all 26 taxa of mammals identified thus far (Qiu and Wang, 1999; Qiu et al., 2006, 2013a; Qiu and Li, 2016).

Baogeda Ula Fauna was initially correlated with Shala Fauna because both of them share many genera in common (Qiu and Wang, 1999). However, updated biochronological results revealed that Baogeda Ula Fauna actually is of a younger age than the Shala Fauna in having some newcomers (e.g., Muridae, Leporidae) and in lacking some archaic elements (e.g., *Midyromys*, *Pentabuneomys*) (Qiu et al., 2013a). Additionally, several genera (*Paralactaga*, *Microtoscopes* and *Ochotona*) in Baogeda Ula Fauna show more advanced features than those from Shala Fauna (Qiu et al., 2006). Considering the presence of the primitive *Hansdebruijnia* and the earliest occurrence of *Parasoriculus*, *Dipoides*, *Microtoscopes*, *Abudhabia*, *Pararhizomys* and *Alilepus* (Table 4) (Mein, 1999; Storch and Ni, 2002; Qiu et al., 2013a), Baogeda Ula Fauna was assigned to the early Baodean (Late Miocene) (Qiu et al., 2013a) of Neogene Chinese Stage/Age and correlated to the MN 12 (middle Turolian) (Qiu et al., 2006, 2013a) of Neogene European Land Mammal zone.

5.3. Correlation of the recognized magnetozones to the ATNTS2012

The faunal assemblage of the Baogeda Ula is comparable with that of the MN 12 unit in Europe. The MN (Mammal Neogene) system established by Mein (1975) has proved very useful and feasible to

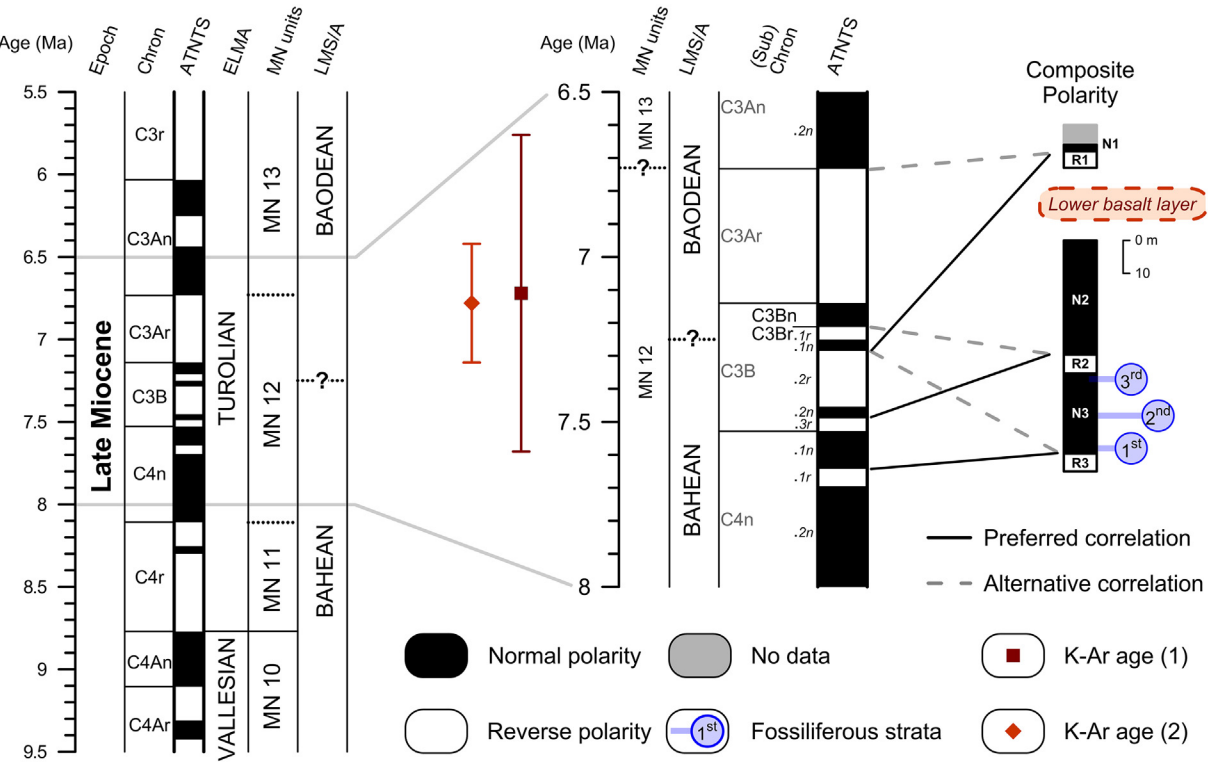


Fig. 9. Correlations of the composite magnetic polarity sequences of Baogeda Ula sections to the Astronomically Tuned Neogene Time Scale (ATNTS) (Hilgen et al., 2012), European Land Mammal Ages (ELMA) and Mammal Neogene (MN) units (Steininger, 1999) and Chinese Neogene Land Mammal Stages/Ages (LMS/A) (Qiu et al., 2013b). Data of K-Ar age (1) is from Luo and Chen (1990), and K-Ar age (2) is from Zhang and Guo (2016).

mammalian faunal correlation across the Europe during the last few decades. Although there is still a debate over the timing and duration of MN 12 (e.g., Krijgsman et al., 1996; Steininger, 1999; Agustí et al., 2001), the end time of MN 12 was thought to be earlier than chron C3An.2n.

In northern China, the Baogeda Ula Fauna is comparable to the famous Baode Fauna. More specifically, the age of the Baogeda Ula Fauna is slightly older than that of the Baode Fauna. Both of them were assigned early Baodean ages. The name of Chinese Baodean Stage/Age derives from Baode County in Shanxi Province of northern China. The ages of the Baode Fauna, which is also characterized by *Hipparrison*, have been palaeomagnetically dated by different researchers. Yue et al. (2004) identified two fossiliferous layers from Jijiagou section. The age of the main fossiliferous strata (the lower layer) is about 7.21–6.73 Ma (from chron C3Bn to C3Ar). Zhu et al. (2008) obtained the ages of three fossiliferous layers from three sections in the same area. Their work placed the age of the oldest fauna within chron C3Br.2r, with a time span of about 7.45–7.28 Ma (Qiu et al., 2013b). Recent study performed by Kaakinen et al. (2013) also suggested that there are at least three fossiliferous levels in Baode area. They provided an estimated age of about 7 Ma (within chron C3Ar) for the oldest fossil localities.

The precise chronological anchor points derived from the lower capping basalt layer and the Baode Faunas support two candidate correlations to the ATNTS2012 (Hilgen et al., 2012) (Fig. 9). We prefer to correlate N3 to chron C4n.1n, and assign N2, including the normal polarity obtained from the lower basalt layer, to chron C3Br.2n (solid lines in Fig. 9). The coarser grainsize of the upper part of sections NEB and ND (Fig. 8), which implies a faster depositional rate, can explain a longer magnetozone N2 compared with N3. This preferred correlation is also supported by the reasonable average sediment accumulation rate (SAR), which is ~19.6 cm/ka, of the section below the lower basalt layer (Supplementary Fig. S2). The normal polarity N1 between two basalt layers could correspond to chron C3Br.1n. Thus, our preferred correlation restricts the age of Baogeda Ula Fauna, which is represented

by three fossiliferous horizons near Baogeda Ula Sumu, within chron C4n.1n with a time span of 7.642–7.528 Ma (Hilgen et al., 2012).

There is an alternative correlation base on the magnetostratigraphic results (dashed lines in Fig. 9). The two normal polarities, N2 and N3, might be correlated to chronos C3Bn and C3Br.1n, respectively. The two short reversed polarities R2 and R3 correspond to chron C3Br.1r and the upper part of chron C3Br.2r, respectively. The two polarities between two basaltic sheets, N1 and R1, may correspond to the beginning of chron C3An and the end of chron C3Ar, respectively. The resultant faunal ages were restricted within chron C3Br.1n with age estimates of 7.285–7.251 Ma (Hilgen et al., 2012). Although both of the two correlations are within the error ranges of the radiometric dates of the capping basalt layer, the alternative correlation yields a slightly younger age for the Baogeda Ula Fauna compared with the oldest Baode Fauna by far (Zhu et al., 2008; Qiu et al., 2013b) and dramatic variations of sedimentation rates (from 73.5 cm/ka to 12.8 cm/ka, see Supplementary Fig. S2).

6. Conclusions

The Baogeda Ula Fauna in central Inner Mongolia, northern China, was previously regarded as an early Baodean fossil assemblage based on biochronological comparison and K-Ar ages of the capping basalt above the fossiliferous strata. The magnetostratigraphic result of the fluvio-lacustrine deposits of the upper Baogeda Ula Formation reveals predominantly normal polarities. Combined with published bio- and geochronological data, our magnetostratigraphic pattern is confidently correlated to the range from chron C4n.1r to chron C3Br.2n of the ATNTS2012. The Baogeda Ula Fauna, including three fossiliferous horizons, can be placed within chron C4n.1n (7.642–7.528 Ma) of latest Tortonian Stage. With the combined magnetostratigraphic and radiometric constraints, the Baogeda Ula Fauna represents an anchor point in biochronology that will contribute to a better understanding of the land mammal biostratigraphy and to the improvement of the Neogene land

mammal biochronological system in northern China.

Supplementary data to this article can be found online at <https://doi.org/10.1016/j.palaeo.2018.06.001>.

Acknowledgments

We thank Dr. Zhuding Qiu from IVPP, Chinese Academy of Sciences for the helpful discussions. Paleomagnetic measurements were made in the Paleomagnetism and Geochronology Laboratory (PGL) of the Institute of Geology and Geophysics, Chinese Academy of Sciences, Beijing. This research was supported by the National Natural Science Foundation of China (grants 41504058, 41688103, 41621004 and L1524016). J.S. Nie, V.A. Kravchinsky and the editor Paul Hesse provided valuable suggestions that substantially improved this manuscript.

References

- Agustí, J., Cabrera, L., Garcés, M., Krijgsman, W., Oms, O., Parés, J.M., 2001. A calibrated mammal scale for the Neogene of Western Europe: state of the art. *Earth Sci. Rev.* 52, 247–260. [http://dx.doi.org/10.1016/S0012-8252\(00\)00025-8](http://dx.doi.org/10.1016/S0012-8252(00)00025-8).
- All-China Stratigraphic Commission, 2017. *Stratigraphic Guide of China and its Explanation*. Geological Publishing House, Beijing (in Chinese).
- Andersson, J.G., 1923. Essays on the Cenozoic of northern China. *Mem. Geol. Surv. Chin. A* 3, 1–152.
- Andrews, R.C., 1932. The new conquest of Central Asia: a narrative of the explorations of the Central Asiatic Expeditions in Mongolia and China, 1921–1930. In: *Natural History of Central Asia*. Vol. 1 American Museum of Natural History, New York. <http://dx.doi.org/10.5962/bhl.title.12200>.
- Bureau of Geology and Mineral Resources of Nei Mongol Autonomous Region, 1991. *Regional geology of Nei Mongol (Inner Mongolia) autonomous Region*. In: *Geological Memoirs Series 1. Geological Publishing House, Beijing* (in Chinese).
- Day, R., Fuller, M.D., Schmidt, V.A., 1977. Hysteresis properties of titanomagnetites: grain size and composition dependence. *Phys. Earth Planet. Inter.* 13 (4), 260–267. [http://dx.doi.org/10.1016/0031-9201\(77\)90108-X](http://dx.doi.org/10.1016/0031-9201(77)90108-X).
- Deng, T., 2006. Chinese Neogene mammal biochronology. *Vertebrata PalAsiatica* 44 (2), 143–163.
- Deng, F.L., MacDougall, J.D., 1992. Proterozoic depletion of the lithosphere recorded in mantle xenoliths from Inner Mongolia. *Nature* 360, 333–336. <http://dx.doi.org/10.1038/360333a0>.
- Deng, C.L., Zhu, R.X., Zhang, R., Ao, H., Pan, Y.X., 2008. Timing of the Nihewan formation and faunas. *Quat. Res.* 69, 77–90. <http://dx.doi.org/10.1016/j.yqres.2007.10.006>.
- Deng, T., Wang, H., Wang, X., Li, Q., Tseng, Z.J., 2016. The Late Miocene *Hipparrison* (Equidae, Perissodactyla) fossils from Baogeda Ula, Inner Mongolia, China. *Hist. Biol.* 28 (1–2), 53–68. <http://dx.doi.org/10.1080/08912963.2015.1020425>.
- Deng, C.L., Hao, Q.Z., Guo, Z.T., Zhu, R.X., 2018a. Quaternary integrative stratigraphy and timescale of China. *Sci. China Earth Sci.* 61. <http://dx.doi.org/10.1007/s11430-017-9195-4>.
- Deng, T., Hou, S., Wang, S., 2018b. Neogene integrative stratigraphy and timescale of China. *Sci. China Earth Sci.* 61. <http://dx.doi.org/10.1007/s11430-017-9155-4>.
- Ding, Z.L., Sun, J.M., Liu, T.S., Zhu, R.X., Yang, S.L., Guo, B., 1998. Wind-blown origin of the Pliocene red clay formation in the central Loess Plateau, China. *Earth Planet. Sci. Lett.* 161, 135–143. [http://dx.doi.org/10.1016/S0012-821X\(98\)00145-9](http://dx.doi.org/10.1016/S0012-821X(98)00145-9).
- Fisher, R., 1953. Dispersion on a sphere. *Proc. R. Soc. London, Ser. A* 217, 295–305. <http://dx.doi.org/10.1098/rspa.1953.0064>.
- Guo, Z.T., Ruddiman, W.F., Hao, Q.Z., Wu, H.B., Qiao, Y.S., Zhu, R.X., Peng, S.Z., Wei, J.J., Yuan, B.Y., Liu, T.S., 2002. Onset of Asian desertification by 22 Myr ago inferred from loess deposits in China. *Nature* 416, 159–163. <http://dx.doi.org/10.1038/416159a>.
- Hilgen, F.J., Lourens, L.J., Van Dam, J.A., 2012. The Neogene Period. In: Gradstein, F.M., Ogg, J.G., Schmitz, M.D., Ogg, G.M. (Eds.), *The Geologic Time Scale 2012*. Vol. 2. Elsevier, Amsterdam, pp. 923–978. <http://dx.doi.org/10.1016/B978-0-444-59425-9.01001-5>.
- Ho, K.S., Liu, Y., Chen, J.C., Yang, H.J., 2008. Elemental and Sr-Nd-Pb isotopic compositions of late Cenozoic Abaga Basalts, Inner Mongolia: implications for petrogenesis and mantle process. *Geochim. J.* 42, 339–357. <http://dx.doi.org/10.2343/geochemj.42.339>.
- Kaakinen, A., Passey, B.H., Zhang, Z.Q., Liu, L.P., Pesonen, L.J., Fortelius, M., 2013. Stratigraphy and paleoecology of the classical dragon bone localities of Baode County, Shanxi Province. In: Wang, X.M., Flynn, L.J., Fortelius, M. (Eds.), *Fossil Mammals of Asia: Neogene Biostratigraphy and Chronology*. Columbia University Press, New York, pp. 203–217. <http://dx.doi.org/10.7312/wang15012>.
- Kaakinen, A., Aziz, H.A., Passey, B.H., Zhang, Z.Q., Liu, L.P., Salminen, J., Wang, L.H., Krijgsman, W., Fortelius, M., 2015. Age and stratigraphic context of *Pliopithecus* and associated fauna from Miocene sedimentary strata at Damiao, Inner Mongolia, China. *J. Asian Earth Sci.* 100, 78–90. <http://dx.doi.org/10.1016/j.jseas.2014.12.014>.
- Kirschvink, J.L., 1980. The least-squares line and plane and the analysis of palaeomagnetic data. *Geophys. J. R. Astron. Soc.* 62, 699–718. <http://dx.doi.org/10.1111/j.1365-246X.1980.tb02601.x>.
- Kononova, V.A., Kurat, G., Embey-Isztin, A., Pervov, V., Koeberl, A.C., Brandstätter, F., 2002. Geochemistry of metasomatised spinel peridotite xenoliths from the Dariganga Plateau, South-eastern Mongolia. *Mineral. Petrol.* 75, 1–21. <http://dx.doi.org/10.1007/s007100200012>.
- Krijgsman, W., Garcés, M., Langereis, C.G., Daams, R., van Dam, J., van der Meulen, A.J., Agustí, J., Cabrera, L., 1996. A new chronology for the middle to late Miocene continental record in Spain. *Earth Planet. Sci. Lett.* 142, 367–380. [http://dx.doi.org/10.1016/0012-821X\(96\)00109-4](http://dx.doi.org/10.1016/0012-821X(96)00109-4).
- Li, Q., 2010. *Parahizomys (Rodentia, Mammalia) from the Late Miocene of Baogeda Ula, central Nei Mongol*. *Vertebrata PalAsiatica* 48 (1), 48–62.
- Liddicoat, J., Wang, X.M., Qiu, Z.D., Li, Q., 2007. Recent palaeomagnetic and magnetostratigraphic investigations on and around the Tunggur tableland, central Nei Mongol (Inner Mongolia). *Vertebrata PalAsiatica* 45 (2), 110–117.
- Lowrie, W., 1990. Identification of ferromagnetic minerals in a rock by coercivity and unblocking temperature properties. *Geophys. Res. Lett.* 17 (2), 159–162. <http://dx.doi.org/10.1029/GL017i002p00159>.
- Luo, X.Q., Chen, Q.T., 1990. Preliminary study on geochronology for Cenozoic basalts from Inner Mongolia. *Acta Petrol. Mineral.* 9 (1), 37–68 (in Chinese with English abstract).
- Mein, P., 1975. Résultats du groupe de travail des vertébrés: biozonation du Néogène méditerranéen à partir des mammifères. In: Senès, J. (Ed.), *Report on Activity of the Regional Committee on Mediterranean Neogene Stratigraphy Working Groups (1971–1975)*, pp. 78–81 (Bratislava).
- Mein, P., 1999. European Miocene mammal biochronology. In: Rössner, G.E., Heissig, K. (Eds.), *The Miocene Land Mammals of Europe*. Verlag Dr. Friedrich Pfeil, Munich, pp. 25–38.
- O'Connor, J., Prothero, D.R., Wang, X.M., Li, Q., Qiu, Z.D., 2008. Magnetic stratigraphy of the Lower Pliocene Gaoteghe beds, Inner Mongolia. *N. M. Mus. Nat. Hist. Sci. Bull.* 44, 431–436.
- Qiu, Z.D., Li, C.K., 2005. Evolution of Chinese mammalian faunal regions and elevation of the Qinghai-Xizang (Tibet) Plateau. *Sci. China Ser. D Earth Sci.* 48 (8), 1246–1258. <http://dx.doi.org/10.1360/03y05023>.
- Qiu, Z.D., Li, Q., 2016. Neogene rodents from central Nei Mongol, China. *Acta Palaeontol. Sin.* 198 (30), 1–684 (in Chinese with English summary).
- Qiu, Z.X., Qiu, Z.D., 1995. Chronological sequence and subdivision of Chinese Neogene mammalian faunas. *Palaeogeogr. Palaeoclimatol. Palaeoecol.* 116, 41–70. [http://dx.doi.org/10.1016/0031-0182\(94\)00095-P](http://dx.doi.org/10.1016/0031-0182(94)00095-P).
- Qiu, Z.D., Wang, X.M., 1999. Small mammal faunas and their ages in Miocene of central Nei Mongol (Inner Mongolia). *Vertebrata PalAsiatica* 37 (2), 120–139 (in Chinese with English abstract).
- Qiu, Z.D., Wang, X.M., Li, Q., 2006. Faunal succession and biochronology of the Miocene through Pliocene in Nei Mongol (Inner Mongolia). *Vertebrata PalAsiatica* 44 (2), 164–181.
- Qiu, Z.D., Wang, X.M., Li, Q., 2013a. Neogene faunal succession and biochronology of central Nei Mongol (Inner Mongolia). In: Wang, X.M., Flynn, L.J., Fortelius, M. (Eds.), *Fossil Mammals of Asia: Neogene Biostratigraphy and Chronology*. Columbia University Press, New York, pp. 155–186. <http://dx.doi.org/10.7312/wang15012>.
- Qiu, Z.X., Qiu, Z.D., Deng, T., Li, C.K., Zhang, Z.Q., Wang, B.Y., Wang, X.M., 2013b. Neogene land mammal stages/ages of China: toward the goal to establish an Asian land mammal stage/age scheme. In: Wang, X.M., Flynn, L.J., Fortelius, M. (Eds.), *Fossil Mammals of Asia: Neogene Biostratigraphy and Chronology*. Columbia University Press, New York, pp. 29–90. <http://dx.doi.org/10.7312/wang15012>.
- Steininger, F.F., 1999. *Chronostratigraphy, geochronology and biochronology of the Miocene “European Land Mammal Mega-Zones” (ELMMZ) and the Miocene “Mammal-Zones (MN-Zones)”*. In: Rössner, G.E., Heissig, K. (Eds.), *The Miocene Land Mammals of Europe*. Verlag Dr. Friedrich Pfeil, Munich, pp. 9–24.
- Storch, G., Ni, X.J., 2002. New Late Miocene murids from China (Mammalia, Rodentia). *Geobios* 35, 515–521. [http://dx.doi.org/10.1016/S0016-6995\(02\)00043-8](http://dx.doi.org/10.1016/S0016-6995(02)00043-8).
- Teilhard de Chardin, P., 1926. *Déscription de mammifères tertiaires de Chine et de Mongolie*. *Ann. Paleontol.* 15, 1–52.
- Tseng, Z.J., Wang, X.M., 2007. The first record of the Late Miocene *Hyaenictitherium Hyaeoidea* Zdansky (Carnivora: Hyaenidae) in Inner Mongolia and an evaluation of the genus. *J. Vertebr. Paleontol.* 27 (3), 699–708. [http://dx.doi.org/10.1671/0272-4634\(2007\)27\[699:TFROT\]2.0.CO;2](http://dx.doi.org/10.1671/0272-4634(2007)27[699:TFROT]2.0.CO;2).
- Wang, P.X., 1990. Neogene stratigraphy and paleoenvironments of China. *Palaeogeogr. Palaeoclimatol. Palaeoecol.* 77, 315–334. [http://dx.doi.org/10.1016/0031-0182\(90\)90183-8](http://dx.doi.org/10.1016/0031-0182(90)90183-8).
- Wang, X.M., Li, P., 2011. A new fossil site with a re-worked Paleogene assemblage at Baogeda Ula, central Nei Mongol. *Vertebrata PalAsiatica* 49 (1), 114–122.
- Wang, X.M., Qiu, Z.D., Opdyke, N., 2003. Litho-, bio-, and magnetostratigraphy and paleoenvironment of Tunggur Formation (middle Miocene) in the Central Inner Mongolia, China. *Am. Mus. Novit.* 3411, 1–31. [http://dx.doi.org/10.1206/0003-0082\(2003\)411<0001:LBAMAP>2.0.CO;2](http://dx.doi.org/10.1206/0003-0082(2003)411<0001:LBAMAP>2.0.CO;2).
- Wang, S., Hu, Y., Wang, L., 2011. New ratite eggshell material from the Miocene of Inner Mongolia, China. *Chinese Birds* 2 (1), 18–26. <http://dx.doi.org/10.5122/cbirds.2011.0002>.
- Wang, X.M., Tseng, Z.J., Takeuchi, G.T., 2012. Zoogeography, molecular divergence, and the fossil record—the case of an extinct fisher, *Pekania palaeosinensis* (Mustelidae, Mammalia), from the Late Miocene Baogeda Ula Formation, Nei Mongol. *Vertebrata PalAsiatica* 50 (3), 293–307.
- Wang, X.M., Flynn, L.J., Fortelius, M., 2013. Toward a continental Asian biostratigraphic and geochronologic framework. In: Wang, X.M., Flynn, L.J., Fortelius, M. (Eds.), *Fossil Mammals of Asia: Neogene Biostratigraphy and Chronology*. Columbia University Press, New York, pp. 1–25. <http://dx.doi.org/10.7312/wang15012>.
- Xu, Y.L., Tong, Y.B., Li, Q., Sun, Z.M., Pei, J.L., Yang, Z.Y., 2007. Magnetostratigraphic dating on the Pliocene mammalian fauna of the Gaoteghe Section, central Inner Mongolia. *Int. Geol. Rev.* 53 (2), 250–260 (in Chinese with English abstract).

- Yue, L.P., Deng, T., Zhang, Y.X., Wang, J.Q., Zhang, R., Yang, L.R., Heller, F., 2004. Magnetostratigraphy of stratotype section of the Baode Stage. *J. Stratigr.* 28, 48–63 (in Chinese with English abstract).
- Zhang, M.L., Guo, Z.F., 2016. Origin of Late Cenozoic Abaga–Dalinuoer basalts, eastern China: implications for a mixed pyroxenite–peridotite source related with deep subduction of the Pacific slab. *Gondwana Res.* 37, 130–151. <http://dx.doi.org/10.1016/j.gr.2016.05.014>.
- Zhu, Y.M., Zhou, L.P., Mo, D.W., Kaakinen, A., Zhang, Z.Q., Fortelius, M., 2008. A new magnetostratigraphic framework for late Neogene *Hippurion* Red Clay in the eastern Loess Plateau of China. *Palaeogeogr. Palaeoclimatol. Palaeoecol.* 268, 47–57. <http://dx.doi.org/10.1016/j.palaeo.2008.08.001>.
- Zijderveld, J.D.A., 1967. A. C. demagnetization of rocks: analysis of results. In: Collinson, D.W., Creer, K.M., Runcorn, S.K. (Eds.), *Methods in Paleomagnetism*. Elsevier, Amsterdam, pp. 254–286.